computation

MDPI

Article

Three-Dimensional Reconstruction of the Right Ventricle from a Radial Basis Morphing of the Inner Surface

Carlotta Fontana * and Nicola Cappetti

Department of Industrial Engineering, University of Salerno, 84084 Fisciano, SA, Italy; ncappetti@unisa.it
* Correspondence: cfontana@unisa.it; Tel.: +39-089-964011

Abstract: In the realm of cardiac health research, accurate fluid dynamics simulations are vital for comprehending the heart function and diagnosing conditions. Central to these simulations is the precision of ventricular wall meshes used to model heart geometry. However, segmenting the wetted surface, particularly in the right ventricle (RV) with its significantly thinner parietal thickness compared to the left ventricle, presents challenges. This study focuses on qualitatively evaluating an automated reconstruction model for the RV's outer wall using Radial Basis function (RBF) morphing. Two procedural criteria were compared, a random selection of control points and a curvature-based approach, which differ in terms of the identification of the control points of the RBF function. From these considerations, it emerges that a controlled use of the RBF function on the basis of the curvatures guarantees the greater controllability of the shape evolutions of the parietal structure of the RV, but it is more sensitive to any anomalies in the distribution of the vertices, as can be seen from the number of outliers, and its controllability is a function of the percentage of points chosen, exerting a greater impact on the required computational capacity. The definition of a strategic criterion for the selection of control points could represent a crucial aspect in the definition of an automatic reconstruction procedure of anatomical elements, which guarantees a morphological variability in line with the need to expand the pathological sample to be used for statistical formulations in the clinical field.

Keywords: right ventricle; radial basis functions; morphing

check for updates

Citation: Fontana, C.; Cappetti, N. Three-Dimensional Reconstruction of the Right Ventricle from a Radial Basis Morphing of the Inner Surface. *Computation* **2024**, *12*, 216. https://doi.org/10.3390/computation12110216

Academic Editor: Jonathan Sinclair

Received: 31 July 2024
Revised: 10 October 2024
Accepted: 25 October 2024
Published: 26 October 2024

Copyright: © 2024 by the authors. Licensee MDPI, Basel, Switzerland. This article is an open access article distributed under the terms and conditions of the Creative Commons Attribution (CC BY) license (https://creativecommons.org/licenses/by/4.0/).

1. Introduction

In the research context of cardiac health, the precision of fluid dynamics simulations plays a pivotal role in understanding the heart function and diagnosing conditions. These simulations rely heavily on the accuracy of the right ventricle (RV) heart wall meshes used to model the heart's geometry.

In the literature, the structural complex of the RV has received a smaller overall number of studies than the left ventricle, due to the difficulty of the segmentation process, owing to multiple factors. In more detail, the presence of ill-defined borders and thin parietal structures prevents the delineation of a clear separation border between one anatomical region and the adjacent one. This result intensifies with the potential disturbances in resolution of the associated diagnostic investigations, including the partial volume effect [1].

Because of these complexities, quantifying the regional myocardium wall thickness is not generally recommended for the cardiac functional analysis of the RV [2].

Compared to the left ventricle, the right ventricle has a wall thickness three times smaller, with values around 3–5 mm [3]. An accurate reconstruction of the wall of cardiac structures constitutes a difficult task but is, nevertheless, essential for the recognition of pathological anomalies, as in the case of muscular hypertrophy and cardiomyopathy [4], as well as for the predictive analysis of reference hemodynamic evolutions subjected to fluid dynamic simulation processes [5]. The scientific community suffers from a difficulty in finding accurate cardiac atlas models of a sufficient sample size to be subjected to fluid dynamic simulations of various kinds [6].

Recent studies have explored the possibility of performing simulations of fluid–structure interaction with an innovative electrical activation of the muscle. These works represent new frontiers in the understanding and modeling of muscle dynamics, but require the use of exact geometries of the heart walls, currently reconstructed on the basis of bibliographical references of a statistical nature, due to the complexity of reconstructing the heart walls starting from the segmentation of diagnostic acquisitions. In their study, Augustin et al. [7] developed a personalized electromechanical modeling framework for the left atrium (LA), which simulates active contraction using patient-specific anatomical finite element meshes with rule-based myofiber directions. They investigated the relationship between wall stress, wall thickness, and curvature in the LA, revealing that wall thickness has a stronger correlation with wall stress than curvature. This finding underscores the importance of accurately reconstructing the wall thickness in heart wall simulations to ensure precise stress estimations. Furthermore, Augustin et al. (2020) demonstrated the limitations of the law of Laplace in estimating local wall stress in the LA, highlighting the need for more complex models that account for anatomy, fiber structures, boundary conditions, and active contraction. These findings emphasize the critical role of thickness reconstruction in heart wall simulations, as it significantly impacts the accuracy of stress estimations and the overall understanding of atrial function and dysfunction.

The work proposed by [8] highlighted the importance of myocardium thickness in the simulation scenario for cardiac radioablation. They found that myocardium thickness is a particularly useful indicator for localizing ventricular tachycardia (VT) sources, which are more visible on cardiac CT scans with contrast agents compared to traditional slice-by-slice representations. The researchers developed a process to automatically infer the myocardium thickness from a cardiac CT scan segmentation, projecting this information onto a 3D mesh for incorporation into the simulation. The thickness information was crucial in generating the target volume delineated on the left ventricle's surface. This approach was compared to a standard slice-by-slice delineation with mental electroanatomical mapping (EAM) registration. The main finding is that incorporating myocardium wall thickness information derived from cardiac CT scan segmentation played a significant role in defining the target volume for the simulated delineation process. This method enabled a more accurate representation of the target volume compared to the classical 2D slice-by-slice approach.

These findings underscore the importance of incorporating myocardium wall thickness information in cardiac simulations to improve the accuracy of target volume delineation and enhance the overall effectiveness of cardiac radioablation procedures.

To date, only a few studies have reported a critical investigation of thickness reconstruction accuracy in heart wall simulations, especially in reference to the right ventricle. In more detail, there is an evident difficulty in automating the segmentation of the wall thicknesses of the ventricular regions, with respect to the related wetted surfaces. This condition is justified by the fact that the contrast medium injected during the diagnostic acquisition phase highlights the surface in contact with the blood, facilitating the process of delimiting the contour of the internal wall, a condition which is not applicable to the outermost thickness contour, making its recognition less remarkable in the first phase of the visual analysis of the contrast distribution of the digital image.

This report delves into an analysis of right ventricle external wall reconstruction throughout the use of morphing operations, aiming to evaluate their suitability for accurate fluid dynamics simulations.

One way to reconstruct the external walls of the ventricle automatically is to expand the wetted surface relating to the endocardium by a value extrapolated from the literature, and to do so in a timely manner by generating a surface expansion map in which each vertex relating to the wet surface mesh corresponds to a point offset value. The anatomical adaptation of any cardiac region of reference to a specific patient can take place without incurring the loss of the relative peculiarities of shape or of those physiognomic features that particularize the anatomical condition of each heart under examination, through the

use of local morphing processing. Among these, Radial Basis functions (RBFs) represent a class of interpolation functions capable of guiding the expansion of a discrete surface through the imposition of origin and arrival control points. These functions are widely used in the investigation of anatomical complexes to be subjected to investigative analyses [9,10]. A theoretical clarification of the aforementioned functions can be found in [11].

By scrutinizing the geometric characteristics and modifications applied through RBFs, we seek to identify the optimal mesh configurations for simulating cardiac fluid dynamics. This study focuses on the degree of accuracy of RV thickness reconstruction in two distinct control point selection methodologies, employed within an RBF-based morphing function: a selection of control points starting from a random choice of the vertices of the starting mesh (random points (RP)), and one starting from the identification of areas with greater curvature (curvature points (CP)). The choice of control point selection method can significantly influence the perception of data variability. Through a detailed quantitative analysis, we investigate how the reconstruction accuracy varies in relation to the percentage of the selected control points, using both the RP and CP methods. The objective is to determine which of the two methods shows a greater sensitivity in approximating the ideal surface and how this sensitivity can influence the interpretation of the analytical results.

2. Materials and Methods

2.1. Introduction to RBF Functions

Radial Basis functions represent a class of functions widely used in various areas of computer science and applied mathematics, including interpolation, machine learning, and neural networks. The distinctive feature of an RBF is that its value depends solely on the distance from a central point, making it particularly suitable for modeling nonlinear spatial relationships [12,13].

The morphing RBF function is described by the following formula:

$$f(x) = \sum_{i=1}^{N} w_i * \varphi(||x - c_i||),$$

where n is the number of RBF functions (or control points), w_i is the weight associated with the i-th RBF function, and φ is the RBF function itself, which depends on the Euclidean distance $|(|x - c|)|$ between the input vector x and the center c_i of the i-th RBF function.

- Gaussian: $\varphi(r) = e^{-(\epsilon r)^2}$, where ϵ is a parameter that adjusts the width of the function;
- Multiquadric: $\varphi(r) = \sqrt{1 + (\epsilon r)^2}$;
- Inverse Multiquadric: $\varphi(r) = \frac{1}{\sqrt{1+(\epsilon r)^2}}$.

Control points, or centers, play a crucial role in defining RBF functions. Their selection significantly affects the accuracy of the interpolation or classification achieved. Among the most frequently used selection criteria we find the one based on a uniform distribution, in which the centers are uniformly distributed in space, used in RBF function interpolation to evenly distribute the control points across the input space [14]. A second approach is the Greedy Algorithm type, which selects the centers iteratively, minimizing an error criterion at each step [15].

The implications arising from the choice of control points correlate to multiple factors involved in the quality of the result, such as

- Accuracy: An appropriate selection of control points can significantly improve the accuracy of the interpolation or classification;
- Overfitting: An excessive number of control points can lead to overfitting, reducing the ability to generalize the model;
- Computational cost: The number of checkpoints affects the computational complexity, directly impacting the computation time needed.

RBF functions and control point selection are fundamental elements in interpolation and machine learning. A thorough understanding of these concepts is crucial for the effective implementation of RBF-based algorithms.

In the field of the virtual simulation of cardiac models, the work presented by Xu et al. [16] accurately elucidates the versatility of the RBF in following surface wall time deformations. The method mentioned the importance of control points, but it focuses on a procedural points' interpolation function, without specifying any topological locations choice. Similarly, the work of Weissman et al. [17] validated the potential of morphing functions to reproduce different cardiac patient's models, but with limited attention to the influence of control points within the effects of RBF functions.

The present work intends to test the accuracy of RBF functions in the reconstruction of RV walls by comparing two case studies in which the selection of control points is carried out, respectively, on a random basis (RP) and on the selection of points belonging to areas relevant to the curvature (CP).

The RBF-type morphing method used here refers to the work presented by [18].

2.2. Data Collection and Preparation

This study utilized a 3D reconstruction of the wet surface of RV heart wall mesh derived from high-resolution imaging data. The cardiac model was provided by the work of Viola et al. [6], characterized by its resolution, number of elements, and specific geometric features pertinent to the RV cardiac anatomy (Figure 1a). The resolution of the raw diagnostic scans was about $0.410 \times 0.410 \times 0.625$ mm^3. The 3D model of the RV was comprised of 83,970 vertices, globally. Traditionally, numerical simulations encounter computational and mathematical efforts in solving anatomical dynamics originating from the use of raw segmentation processes [19]. This phenomenon is also more crucial in the segmentation task of reconstructing the RV thickness, due to limited scale dimensions that are even smaller than the diagnostic image pixel spacing (Figure 1b), as depicted by the state of the art. In this sense, with respect to the original conformation of the cardiac inner wall surfaces, normally marked by the presence of undulatory roughness, the model here described underwent a superficial smoothing process, targeting the focus on the manipulation of virtual structures that follow anatomical adherence, without impacting on the effective outcome of the simulation analysis. The new mesh was further generated from the original one, using an RBF function to introduce varying degrees of offset and curvature, simulating different physiological conditions. In more detail, a series of 3D models was generated through RBF approximations, with a selection of control RBF points randomly selected from the original mesh and the curvature selected, respectively, in a percentage variation going from 10% to 90%. The models were compared against a Gold Standard model to assess accuracy.

The reference geometrical model taken as the Gold Standard parameter in the evaluation of the obtained results was generated through an expansion procedure of the original cardiac mesh. In more detail, for each of the total vertices of the wet mesh surface extracted as a result of the diagnostic acquisition segmentation process, a local shift along the normal direction was provided on the basis of thickening behavior drawn from a theoretical bibliography reference [14], distributed along the whole set of vertices by means of an interpolating spatial distribution procedure. The subsequent morphing results were, then, compared in their efficacy evaluation in terms of a point-to-point distance computation from the reference standard thus described, so as to analyze any qualitative change in the performance exhibited by the radial basis morphing procedure for different criteria of selection of control points.

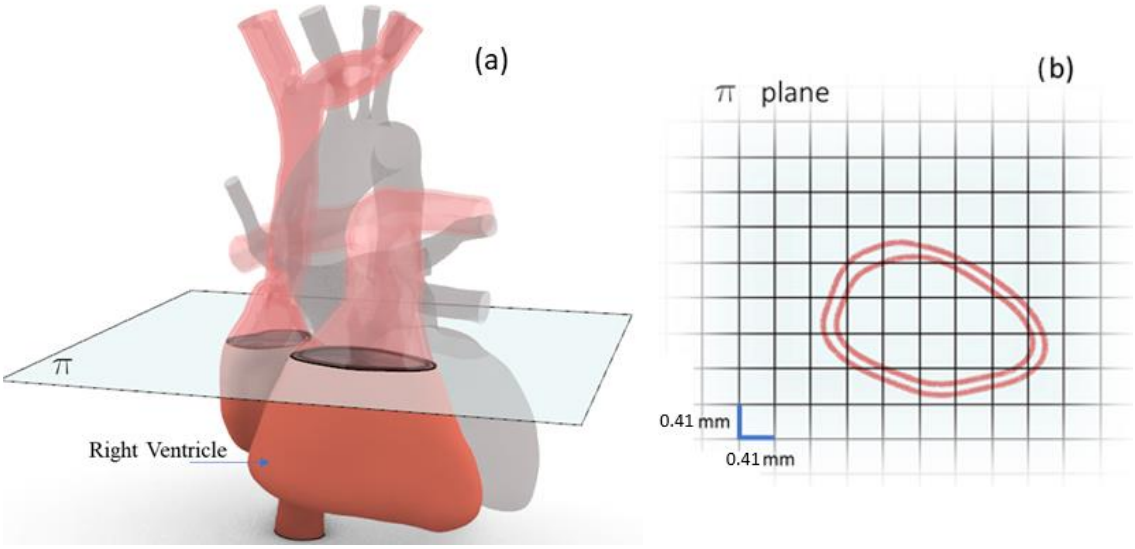

Figure 1. (**a**) Prospective view of the virtual heart model considered. The right cardiac part, evidenced in a red color, displays the right atrium, visible at the upper rear, and the right ventricle, at the bottom front. The clipping plane, p, is representative of a cutting slice from diagnostic acquisition, augmented in (**b**), where it lies along the contour curves of the inner and outer surface of the RV. The slice resolution pixel spacing is enhanced to compare it with the subtle RV wall thickness' small-scale dimensions, complicating the segmentation reconstruction process.

With reference to the control points selection mode to be used in the morphing action, the RP mode defines the RBF control points as a random selection of a defined percentage of the original vertex. In the CP mode, the random selection was again based on the random selection of a defined percentage of the original vertex, weighted by a curvature distribution analysis computed along the entire set of mesh vertices (Dong and Wang, 2005). The effect of the percentage level was analyzed, testing different values from 10% to 90%.

The data for analysis were extracted from the models' distances to the Gold Standard.

3. Results

In this study, we generated three samples of Radial Basis function (RBF) control point selections for each percentage case considered. The goal was to ensure statistical significance by significantly reducing the variance between the samples for each case examined. The results obtained from consulting the statistical indices for each percentage sample strengthened the significance of the analytical evaluations subsequently used. An example case can be seen in Table 1, where the descriptive values of the repeated samples for the CP 20% case are presented.

Table 1. Evaluation of statistical indices of three randomly repeated samples for the CP 20% case.

CP 20%	Sample 1	Sample 2	Sample 3
mean	1.29×10^{-2}	1.05×10^{-2}	1.03×10^{-2}
std	6.21×10^{-2}	3.31×10^{-2}	3.22×10^{-2}
min	0.00×10^{0}	0.00×10^{0}	0.00×10^{0}
25%	7.25×10^{-4}	6.86×10^{-4}	7.30×10^{-4}
50%	3.60×10^{-3}	3.41×10^{-3}	3.60×10^{-3}
75%	1.03×10^{-2}	9.41×10^{-3}	1.00×10^{-2}
max	2.89×10^{0}	1.86×10^{0}	2.43×10^{0}

For each case considered, a measure of the distance from the reference Gold Standard was calculated as the average of the distances of the three samples, in order to characterize

the degree of adherence of each model to the ideal shape to be achieved, evaluating the behavior exhibited by the RBF function when varying control points (Tables 2 and 3).

Table 2. Random points: descriptive statistics for distances between homologous points [mm].

	10%	20%	30%	40%	50%	60%	70%	80%	90%
mean	7.71×10^{-3}	5.27×10^{-3}	4.86×10^{-3}	5.34×10^{-3}	6.24×10^{-3}	6.60×10^{-3}	7.16×10^{-3}	6.90×10^{-3}	5.00×10^{-3}
std	8.93×10^{-3}	5.21×10^{-3}	6.19×10^{-3}	9.24×10^{-3}	1.51×10^{-2}	2.71×10^{-2}	4.29×10^{-2}	7.30×10^{-2}	7.27×10^{-2}
min	2.14×10^{-16}	1.48×10^{-3}	1.32×10^{-16}	4.45×10^{-16}	1.05×10^{-15}	8.92×10^{-15}	8.63×10^{-14}	3.87×10^{-13}	2.53×10^{-12}
25%	2.75×10^{-3}	2.05×10^{-3}	1.43×10^{-3}	1.05×10^{-3}	7.20×10^{-4}	2.87×10^{-4}	1.03×10^{-8}	2.39×10^{-8}	7.47×10^{-8}
50%	4.83×10^{-3}	3.77×10^{-3}	2.89×10^{-3}	2.48×10^{-3}	2.07×10^{-3}	1.48×10^{-3}	8.53×10^{-4}	5.70×10^{-7}	3.26×10^{-7}
75%	8.74×10^{-3}	6.72×10^{-3}	5.79×10^{-3}	5.55×10^{-3}	5.43×10^{-3}	4.52×10^{-3}	3.29×10^{-3}	1.84×10^{-3}	3.08×10^{-4}
max	1.09×10^{-1}	9.04×10^{-2}	9.17×10^{-2}	2.55×10^{-1}	4.79×10^{-1}	2.47×10^{0}	2.54×10^{0}	6.60×10^{0}	6.55×10^{0}

Table 3. Curvature points: descriptive statistics for distances between homologous points [mm].

	10%	20%	30%	40%	50%	60%	70%	80%	90%
mean	6.87×10^{-2}	2.19×10^{-1}	2.78×10^{-2}	2.05×10^{-2}	1.23×10^{-2}	9.95×10^{-3}	8.73×10^{-3}	6.77×10^{-3}	6.10×10^{-3}
std	3.73×10^{-2}	1.52×10^{0}	2.33×10^{-1}	1.75×10^{-1}	8.34×10^{-2}	8.38×10^{-2}	9.97×10^{-2}	9.61×10^{-2}	1.70×10^{-1}
min	2.14×10^{-16}	1.48×10^{-16}	1.32×10^{-16}	4.45×10^{-16}	1.05×10^{-15}	8.92×10^{-15}	8.63×10^{-14}	3.87×10^{-13}	2.53×10^{-12}
25%	2.75×10^{-3}	2.05×10^{-3}	1.43×10^{-3}	1.05×10^{-3}	7.20×10^{-4}	2.87×10^{-4}	1.03×10^{-8}	2.39×10^{-8}	7.47×10^{-8}
50%	4.83×10^{-3}	3.77×10^{-3}	2.89×10^{-3}	2.48×10^{-3}	2.07×10^{-4}	1.48×10^{-3}	8.53×10^{-4}	5.70×10^{-7}	3.26×10^{-7}
75%	2.69×10^{-2}	4.99×10^{-2}	1.45×10^{-2}	8.96×10^{-3}	5.67×10^{-3}	3.36×10^{-3}	1.20×10^{-3}	6.90×10^{-7}	1.61×10^{-6}
max	1.25×10^{-1}	4.58×10^{1}	1.27×10^{1}	8.48×10^{0}	4.34×10^{0}	5.92×10^{0}	1.08×10^{1}	1.41×10^{1}	1.64×10^{1}

The curves shown in Figure 2 provide a representation of the trend of the distance values evaluated in the two cases, as the percentage of control points varies.

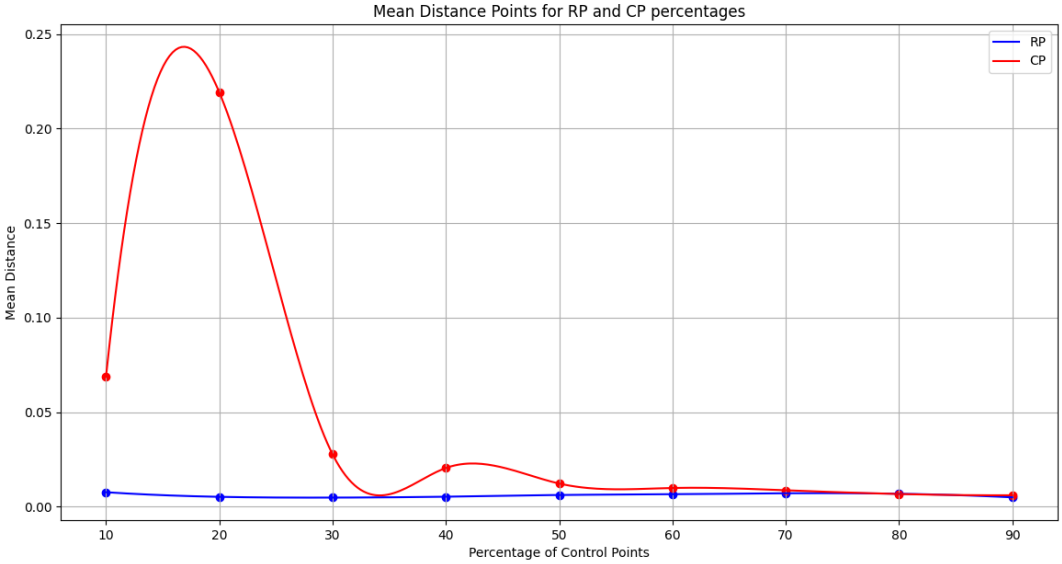

Figure 2. Distribution of the average distances from the Gold Standard for each case considered, curvature points (CP) and random points (RP).

Both curves show how the average distances range as the percentage of control points varies. This helps us better understand the effectiveness of morphing as a function of control point density. The difference between the curves of the averages of the differences relating to the random points and those of the points based on the curvatures highlights the impact of the choice of control points, in particular the effect of the inclusion of points in areas of greater curvature. This suggests that the curvature-based approach could offer advantages in terms of shape adaptation, especially in the presence of complex structures. The analysis shows that the use of control points in areas of greater curvature (the CP approach) can significantly influence the results. Focusing on these areas can improve the adaptation of the morphing to the salient features of cardiac focus, optimizing the quality of the final result.

From the numerical analysis, the percentage of control points that leads to the shortest average distance, according to the CP-type criterion, is equal to 90%, demonstrating an

overall average distance value equal to approximately 6×10^{-3}. This indicates that, for the curvature method, using 90% of the control points minimizes the average distance to the Gold Standard. This suggests that a greater density of control points, concentrated in particular in areas of greater curvature, can significantly improve the adaptation of the morphing to the complex geometric characteristics of the object.

However, the case relating to the selection criterion of control points on the basis of a uniform random selection is different, with the optimal condition for minimizing the average distances from the reference Gold Standard appearing to be located in correspondence with a percentage of points equal to 30%, demonstrating an average value of approximately 5×10^{-3}.

The median of the distances provides an indication of a central tendency that is less sensitive to outliers than the mean. Outlier percentages indicate the proportion of data points that deviate significantly from the median, offering a measure of the variability and consistency of the approximation for each RBF configuration.

RBF functions notably follow mathematical approximations whose behavior is not always stable, so as to determine, sometimes, solutions not geometrically significative. By eliminating outliers, we perform a filtering of this negative outcome, focusing on the central characteristics of the distributions and gaining a clearer view of the overall trend. From the data in Figure 3, we can observe the following trends.

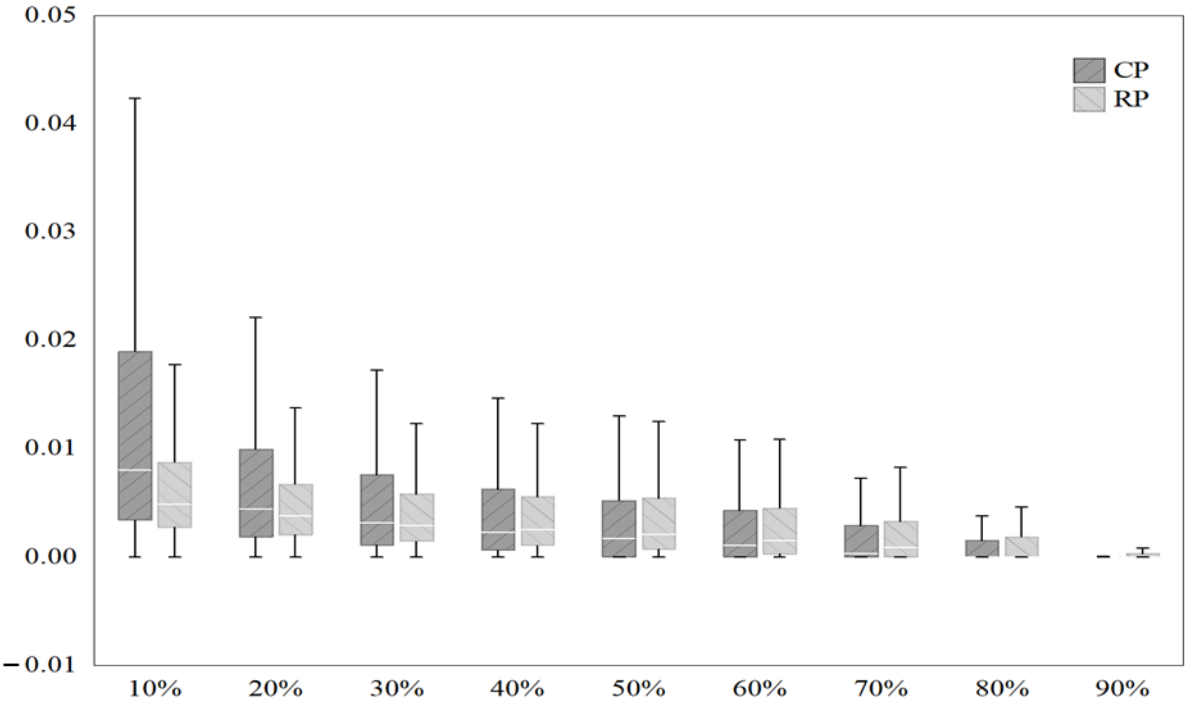

Figure 3. Boxplot distributions of the cases considered, curvature points (CP) and random points (RP), for each percentage of the selected reference points, with the exclusion of outliers.

Medians: Medians represent the central value of the distance distribution for each combination of percentage and method. A lower median indicates a smaller distance from the Gold Standard, suggesting the greater accuracy of the approach.

IQR (Interquartile Range): The IQR measures the variability of the data, indicating the difference between the 25th and 75th percentile. A narrower IQR suggests less variability in distance, indicating more consistent results.

Analyzing the data presented in Table 4, we can see that for the lowest percentages of control points (10–30%), the random point (RP)-based approach tends to have lower medians than the curvature-based approach (CP), suggesting a greater initial accuracy. However, the IQR of the RBF approach shows more variability, especially at 10% and 20%.

Table 4. Tabulated values for medians and interquartile ranges for RP and CP criteria.

Percentage [%]	Method	Median	IQR
10	RP	4.83×10^{-3}	5.99×10^{-3}
	CP	8.96×10^{-3}	2.45×10^{-2}
20	RP	3.77×10^{-3}	4.68×10^{-3}
	CP	1.69×10^{-2}	4.64×10^{-2}
30	RP	2.89×10^{-3}	4.36×10^{-3}
	CP	3.34×10^{-3}	1.45×10^{-2}
40	RP	2.48×10^{-3}	4.50×10^{-3}
	CP	1.55×10^{-3}	8.96×10^{-3}
50	RP	2.07×10^{-3}	4.71×10^{-3}
	CP	2.21×10^{-7}	5.67×10^{-3}
60	RP	1.48×10^{-3}	4.23×10^{-3}
	CP	1.43×10^{-7}	3.36×10^{-3}
70	RP	8.53×10^{-4}	3.29×10^{-3}
	CP	1.31×10^{-7}	1.20×10^{-3}
80	RP	5.70×10^{-7}	1.84×10^{-3}
	CP	1.82×10^{-7}	6.18×10^{-7}
90	RP	3.26×10^{-7}	3.08×10^{-4}
	CP	6.06×10^{-7}	1.38×10^{-6}

As the percentage of control points increases (40–90%), the CP approach shows a notable reduction in both medians and IQR, indicating a significant improvement in the precision and consistency of results. In particular, at higher percentages (70–90%), the CP approach outperforms the RP approach in terms of the median, suggesting greater accuracy in approximating the Gold Standard.

The RP approach shows a general trend of decreasing medians and IQRs as the percentage of control points increases, but the CP approach shows stronger improvements, especially at high percentages. These results suggest that while the random point-based approach may be more effective at lower percentages of control points, the curvature-based approach becomes significantly more precise and consistent at higher percentages, moving closer to the Gold Standard.

For lower percentages (10–30%), the RP method shows generally lower medians than the CP method, indicating a higher initial accuracy.

As we increase the percentage of control points (40–90%), the CP method shows significant improvements in both medians and IQRs, indicating an increase in the precision and consistency of the results.

At higher percentages (70–90%), the CP method outperforms the RP method in terms of the median, suggesting greater accuracy in approximating the Gold Standard.

Removing outliers from the graph helps to focus on the central features of the distributions. However, it is important to remember that outliers can also provide significant information about extreme variations or anomalies in the data. Analyzing how the presence of outliers affects the surface approximation for both methods can help understand which method is more robust to outliers, which is crucial for applications where the data may be subject to noise or measurement errors, as is the case of reconstructions from diagnostic investigations.

In this context, their contribution was reinstated in the statistical analysis of the two criteria adopted, in order to highlight the degree of non-homogeneity in the distribution behavior manifested in the various percentage cases. Below are indicated the percentages of outliers in the two cases, with respect to each percentage:

- RP: [9.4, 5.9, 8.2, 10.2, 11.3, 12.2, 13.6, 14.3, 19.7]

- CP: [11.9, 13.8, 9.4, 12.0, 14.0, 15.2, 18.7, 20.2, 15.0]

From the percentage analysis, we can observe that the percentage of outliers generally increases as the percentage of control points increases for both methods, RP and CP. This suggests that adding more control points can lead to greater variability in distance measurements. The CP method shows a higher percentage of outliers than the RP in many of the control point percentages. This may indicate that curvature-based selection (CP) is more sensitive to variations in the data, leading to greater variability in the measured distances. In more detail, CP shows the highest percentages of outliers at the highest control point percentages, suggesting that the CP methodology may be particularly affected by extreme data when using many control points.

The choice of control points, either randomly or in areas of significant curvature, affects the presence and distribution of outliers in the RBF results. These two conditions reflect different strategies in modeling approach and have distinct implications for the effectiveness and accuracy of the reconstruction. The random selection of control points can lead to a less optimal distribution of points in space, potentially causing greater variability in the reconstruction accuracy. This may result in a greater number of outliers, as some random configurations may not adequately capture the salient features of the data. Outliers in this case may indicate particularly ineffective control point configurations. Selecting control points in areas of significant curvature aims to optimize the effectiveness of the control points by focusing on the areas that contribute most to the overall shape of the function to be approximated. This approach tends to reduce the variability in reconstruction accuracy and, consequently, can lead to fewer outliers. Outliers that occur in this context may reflect the limitations of the RBF model in handling specific geometric or topological characteristics of the data. In terms of outliers, selecting control points in areas of significant curvature tends to be a more robust approach, reducing the likelihood of highly variable results and improving the consistency of reconstruction accuracy. However, the feasibility of this approach depends on the ability to effectively identify such zones, which may require a preliminary analysis or the application domain-specific knowledge.

4. Discussion

In this presented work, the control points' incidence in the effectiveness of a morphing RBF function of the cardiac inner surface to automatically reconstruct the external wall was investigated. Two distinctive choosing methods for control points selection were considered: a curvature-based and a random-based approach. Statistical evaluations were performed, so as to display RBF behavior in multiple configurations, which differed in terms of the percentage of points' density involved in the morphing expansion. Globally, from the estimation of the results data, evaluated we can deduce the following conclusions.

Curvature-based approach: This method selects control points based on the curvature of the data, potentially offering a more accurate representation of salient features of the dataset. With larger datasets, which may have a greater variety of shapes and curvatures, the curvature-based approach may better adapt to the complexities of the data, improving the quality of the RBF reconstruction. However, its effectiveness could be influenced by the specific distribution of the data and by the presence of noise, which is typically considerably present in surfaces obtained from biomedical images that reconstruct organs of small size or thickness.

Randomly selected points approach: This method selects a fixed percentage of control points from the dataset, regardless of the specific characteristics of the data. With small datasets, this approach may be sufficient to capture the essential information needed for good RBF reconstruction. However, as the size of the dataset increases, a random or fixed selection may not be optimal for accurately representing the variety and complexity of the data, potentially resulting in a lower reconstruction quality than the curvature-based approach.

The size of the dataset plays a crucial role in the effectiveness of both approaches. For small datasets, the difference between the two approaches may be less obvious, as

both are able to capture the main characteristics of the data with a limited number of control points. In contrast, for large datasets, the curvature-based approach may show greater effectiveness in capturing data complexities, resulting in a higher reconstruction quality. In conclusion, while the fixed percentage-based approach may be simpler to implement and sufficient for small datasets, the curvature-based approach appears to offer significant advantages for larger datasets, better adapting to the specific characteristics of the data and the relative complexities of shape. The curvature-based approach with a moderate number of control points can represent an advantageous compromise in the morphing process in the presence of complex geometries, resulting in a more effective tracking of shape characteristics, without, however, resulting in a high computational load or in the presence of overfitting. The choice of the most suitable approach could therefore depend on the size of the dataset, as well as its specific characteristics and the objectives of the analysis.

The procedure here presented can offer support to the reconstruction procedure of the walls of the heart, not yet fully consolidated by the scientific literature, to implemented in subsequent fluid dynamic analyses. Through the identification of the optimal control parameters, the reconstruction of the external thickness of cardiac geometries is computationally simplified, starting from the segmentation of the wet surface only, more easily identifiable in the scanning of the diagnostic investigation.

5. Conclusions

The quality of the surface finish plays a decisive role in these studies; surfaces with higher quality finishes tend to positively compromise the accuracy of the simulations, potentially reducing uncertainties related to turbulence and fluid resistance. In this context, the segmentation of the wetted surface emerges as a fundamental process, for which applicable procedures have already been developed that allow the optimizing of the interaction between the fluid and the structure under examination.

The result of this analysis highlights how for a small number of control poles, the function based on a random distribution of points shows a behavior closer to the ideal one, while as the number of control points increases, the selection of regions with a greater curvature affects the reconstruction precision, drastically lowering the distance from the reference Gold Standard. From these considerations, it emerges that a controlled use of the RBF function on the basis of the curvatures guarantees the greater controllability of the shape evolutions of the parietal structure of the RV, but it is more sensitive to any anomalies in the distribution of the vertices, as can be seen from the number of outliers, and its controllability is a function of the percentage of points chosen, exerting a greater impact on the required computational capacity.

Author Contributions: Conceptualization, C.F. and N.C.; methodology, C.F. and N.C.; software, C.F.; validation, C.F. and N.C.; formal analysis, C.F.; investigation, C.F. and N.C.; resources, C.F.; data curation, C.F.; writing—original draft preparation, C.F.; writing—review and editing, C.F. and N.C.; visualization, C.F.; supervision, C.F. and N.C.; project administration, C.F. and N.C. All authors have read and agreed to the published version of the manuscript.

Funding: This research received no external funding.

Data Availability Statement: The raw data supporting the conclusions of this article will be made available by the authors on request.

Acknowledgments: We acknowledge Filippo Caruso for providing the three-dimensional reconstruction of the right ventricle's wet surface and the parietal thickness values interpolation distribution.

Conflicts of Interest: The authors declare no conflicts of interest.

References

1. Petitjean, C.; Zuluaga, M.A.; Bai, W.; Dacher, J.-N.; Grosgeorge, D.; Caudron, J.; Ruan, S.; Ben Ayed, I.; Cardoso, M.J.; Chen, H.-C.; et al. Right Ventricle Segmentation from Cardiac MRI: A Collation Study. *Med. Image Anal.* **2024**, *19*, 187–202. [CrossRef] [PubMed]
2. Peng, P.; Lekadir, K.; Gooya, A.; Shao, L.; Petersen, S.E.; Frangi, A.F. A review of heart chamber segmentation for structural and functional analysis using cardiac magnetic resonance imaging. *Magn. Reson. Mater. Phys. Biol. Med.* **2016**, *29*, 155–195. [CrossRef] [PubMed]
3. Thounaojam, K.; Devi, K.A.; Tunglut, J. Difference in Thickness Between Right Ventricle and Left Ventricle of Adult Human Heart: A Cadaveric Study. *Int. J. Anat. Res.* **2021**, *9*, 8116–8119. [CrossRef]
4. Goo, H.W. Right Ventricular Mass Quantification Using Cardiac CT and a Semiautomatic Three-Dimensional Hybrid Segmentation Approach: A Pilot Study. *Korean J. Radiol.* **2021**, *22*, 901–911. [CrossRef] [PubMed]
5. Mosbahi, S.; Mickaily-Huber, E.; Charbonnier, D.; Hullin, R.; Burki, M.; Ferrari, E.; von Segesser, L.K.; Berdajs, D.A. Computational fluid dynamics of the right ventricular outflow tract and of the pulmonary artery: A bench model of flow dynamics. *Interact. Cardiovasc. Thorac. Surg.* **2014**, *19*, 611–616. [CrossRef] [PubMed]
6. Viola, F.; Del Corso, G.; De Paulis, R.; Verzicco, R. GPU accelerated digital twins of the human heart open new routes for cardiovascular research. *Sci. Rep.* **2023**, *13*, 8230. [CrossRef] [PubMed]
7. Augustin, C.M.; Fastl, T.E.; Neic, A.; Bellini, C.; Whitaker, J.; Rajani, R.; O'neill, M.D.; Bishop, M.J.; Plank, G.; Niederer, S.A. The impact of wall thickness and curvature on wall stress in patient-specific electromechanical models of the left atrium. *Biomech. Model Mechanobiol.* **2020**, *19*, 1015–1034. [CrossRef] [PubMed]
8. Rigal, L.; Benali, K.; Barré, V.; Bougault, M.; Bellec, J.; De Crevoisier, R.; Martins, R.; Simon, A. Multimodal fusion workflow for target delineation in cardiac radioablation of ventricular tachycardia. *Med. Phys.* **2024**, *51*, 292–305. [CrossRef] [PubMed]
9. Pascoletti, G.; Aldieri, A.; Terzini, M.; Bhattacharya, P.; Calì, M.; Zanetti, E.M. Stochastic PCA-based bone models from inverse transform sampling: Proof of concept for mandibles and proximal femurs. *Appl. Sci.* **2021**, *11*, 5204. [CrossRef]
10. Yuan, Q.; Jiang, B.; Zhu, X.; Hu, J.; Wang, Y.; Chou, C.C.; Xu, S. A fast methodology for generating skeletal FEM with detailed human geometric features based on CPD and RBF algorithms. *Sci. Rep.* **2023**, *13*, 8864. [CrossRef] [PubMed]
11. Powell, M.J.D. Radial Basis Functions for Multivariable Interpolation: A Review. *Front. Synaptic. Neurosci.* **2010**, *2*, 143–167.
12. Biancolini, M.E.; Chiappa, A.; Cella, U.; Costa, E.; Groth, C.; Porziani, S. *Radial Basis Functions Mesh Morphing*; Springer: Berlin/Heidelberg, Germany, 2020. [CrossRef]
13. Chen, W.; Fu, Z.J.; Chen, C.S. Radial Basis Functions. In *Recent Advances in Radial Basis Function Collocation Methods*; SpringerBriefs in Applied Sciences and Technology; Springer: Berlin/Heidelberg, Germany, 2014. [CrossRef]
14. Li, M.; Chen, C.; Hon, Y.; Wen, P. Finite integration method for solving multi-dimensional partial differential equations. *Appl. Math. Model.* **2015**, *39*, 4979–4994. [CrossRef]
15. Chen, S.; Cowan, C.F.N.; Grant, P.M. Orthogonal Least Squares Learning Algorithm for Radial Basis Function Networks. *IEEE Trans. Neural. Netw.* **1991**, *2*, 302–309. [CrossRef] [PubMed]
16. Xu, F.; Kenjereš, S. Numerical simulations of flow patterns in the human left ventricle model with a novel dynamic mesh morphing approach based on radial basis function. *Comput. Biol. Med.* **2021**, *130*, 104184. [CrossRef]
17. Weissmann, J.; Charles, C.J.; Richards, A.M.; Yap, C.H.; Marom, G. Cardiac mesh morphing method for finite element modeling of heart failure with preserved ejection fraction. *J. Mech. Behav. Biomed. Mater.* **2022**, *126*, 104937. [CrossRef] [PubMed]
18. Forti, D.; Rozza, G. Efficient geometrical parametrisation techniques of interfaces for reduced-order modelling: Application to fluid–structure interaction coupling problems. *Int. J. Comut. Fluid Dyn.* **2014**, *28*, 158–169. [CrossRef]
19. Bertagna, L.; D'Elia, M.; Perego, M.; Veneziani, A. Data Assimilation in Cardiovascular Fluid–Structure Interaction Problems: An Introduction. *Fluid-Struct. Interact. Biomed. Appl.* **2014**, *2014*, 395–481. [CrossRef]

Disclaimer/Publisher's Note: The statements, opinions and data contained in all publications are solely those of the individual author(s) and contributor(s) and not of MDPI and/or the editor(s). MDPI and/or the editor(s) disclaim responsibility for any injury to people or property resulting from any ideas, methods, instructions or products referred to in the content.